Time–Modulated Antenna Array with Lossless Switching Network

Grzegorz Bogdan, *Student Member, IEEE,* Yevhen Yashchyshyn, *Senior Member, IEEE,* and Miłosz Jarzynka, *Student Member, IEEE*

***Abstract*—In this paper a novel architecture for a time–modulated antenna array (TMAA) based on single–pole double–throw (SPDT) switches is presented. The proposed TMAA has lossless switching network because there is no power loss during the OFF state. In addition to improved efficiency, this TMAA provides beam–scanning capabilities. Moreover, the proposed TMAA has a constant instantaneous directivity, which is favorable for some applications. The architecture has been implemented as an aperture–coupled patch antenna array and verified as a smart antenna in a digital wireless communication system.**

***Index Terms*—wireless communication, antennas, antenna arrays, beam steering, adaptive arrays, interference cancellation.**

I. Introduction

A TIME–MODULATED antenna array (TMAA) is based on periodical ON/OFF switching of signals received/transmitted from/to each antenna array element; hence, continuous wave signals are modulated to pulsed RF signals. The spectrum of a signal after time–modulation is composed of a carrier component and harmonic components (sidebands). When a TMAA is used to receive a signal at the carrier frequency f_0, and the switching frequency $f_p \ll f_0$, sideband components will appear in the receiver. The carrier component can be used for sidelobe reduction [1], while siedebands are suitable for beam–scanning [2], [3].

The advantage of TMAAs lies in beamforming, which is achieved with switches instead of phase–shifters. RF switches based on semiconductors can be low–cost and high power handling components operating in high frequency range [4]. This advantage might be a key factor enabling TMAAs to be a low–cost solution applicable to future intelligent antenna systems for mm–wave communication [5].

The gain of TMAAs depends on two factors: the gain of an array itself (without switching) and the feed network efficiency determined by the losses in an absorptive switches [6], [7]. One of the most common TMAA architecture proposed for potential usage in direction finding [8], interference nulling [9], [10] or a cognitive radio [11] involves absorptive switches, which decrease the overall efficiency due to the power dissipation in the OFF state [6], [7]. This problem has been addressed before, and brought new architectures of TMAAs with SP3T and SPDT switches connected to a pair of array elements [12], [13]. SP3T switches have been used to develop a two–channel TMAA with beam–scanning; the overall efficiency is, however, low due to power losses during the OFF state. On the other hand, a linear TMAA without power loss during the OFF state has been developed, but without flexible capabilities of the radiation pattern reconfiguration [13]. The TMAA presented in this article combines both the advantages outlined above: it has maximum switching network efficiency without losses during the OFF state, and provides beam–scanning capabilities. To the authors' knowledge, such an architecture of TMAA has not been published before.

The paper is organized as follows. Section II describes a new architecture of TMAA and a related method of time–modulation. Section III presents results of the radiation pattern measurement and the interference cancellation performance. Finally, conclusions are drawn in Section IV.

G. Bogdan, Y. Yashchyshyn and M. Jarzynka are with the Institute of Radioelectronics and Multimedia Technology, Warsaw University of Technology, Nowowiejska 15/19, 00–665 Warsaw, Poland (e-mail: g.bogdan@ire.pw.edu.pl, y.yashchyshyn@ire.pw.edu.pl, m.jarzynka@stud.elka.pw.edu.pl).

II. Proposed TMAA architecture

Two linear arrays of length N are placed along the y–axis. Each pair of elements along the x–axis is connected to an SPDT switch. One line is connected to switches via fixed phase–shifters, which enable harmonic beam–scanning on the odd sidebands [14]. A diagram of the proposed architecture is presented in Fig. 1.

The SPDT switch has two positions and does not have an idle (OFF) state. Hence, only one element in each pair can be active. When one element has to be turned OFF, the switch changes its position and excites the adjacent element. Hence, microwave power is not dissipated during the OFF state, but it is delivered to an another element. Moreover, the proposed TMAA has always constant instantaneous directivity [15], because at any time exactly four elements are turned ON.

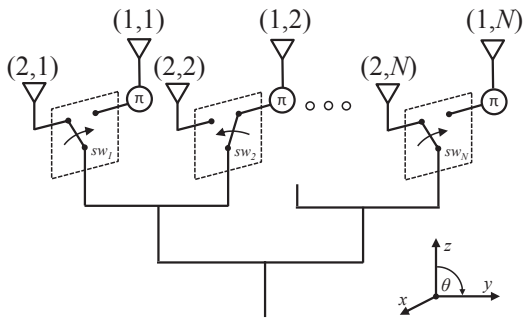

Fig. 1. Diagram of proposed TMAA.

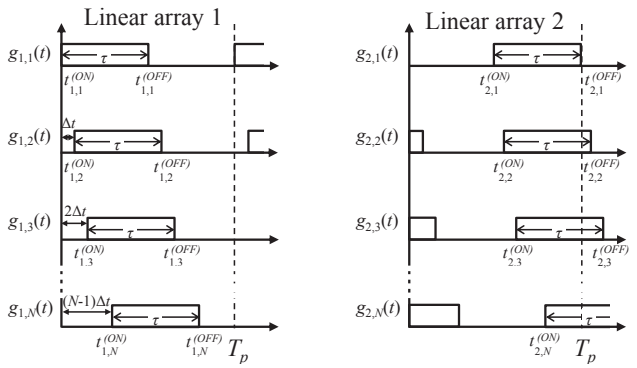

Fig. 2. Modulating signals $g_{m,n}(t)$.

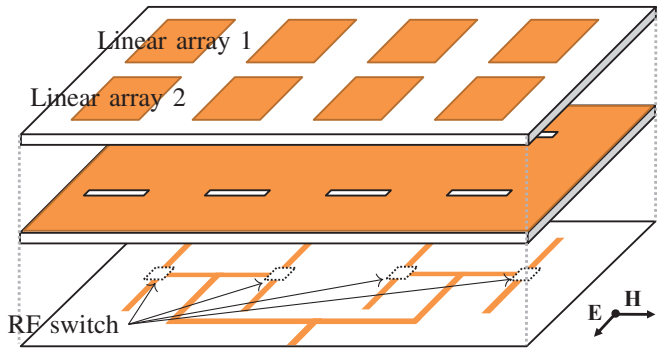

Fig. 3. Structure of aperture–coupled patch antenna array with SPDT switches.

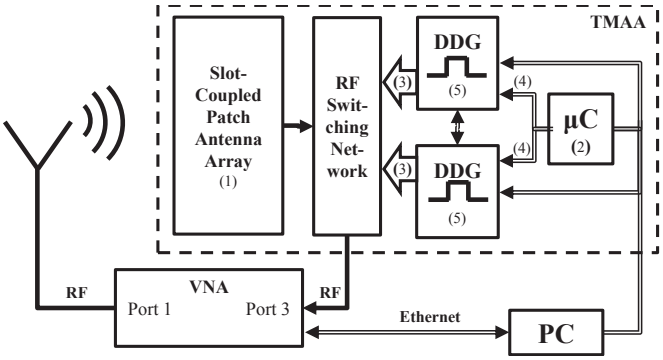

Fig. 4. Diagram of setup for radiation pattern measurements; (1) aperture–coupled patch antenna array, (2) microcontroller, (3) switch control, (4) trigger input, (5) digital delay generator.

Although different methods of switching can be applied, in this paper we propose a delayed half-by-half switching, i.e. two elements within each pair are active for a half of the switching period T_p, where the switching is progressively delayed. The ON/OFF switching is presented in Fig. 2 as rectangular functions $g_{m,n}(t)$ with constant ON–time duration $\tau = T_p/2$ and progressive delay $(n-1)\Delta t$. According to the Fourier series property, even components are not present if the duty cycle of rectangular waveform equals $50\,\%$. This doubles the spacing between sidebands and relaxes the restriction on maximum signal bandwidth [16]. Parameter Δt can be modified to control the array factor and perform beamforming.

Fixed $180°$ phase–shifters placed between two linear arrays compensate phase–difference on odd sidebands.

To evaluate beam–scanning properties of the proposed architecture, an aperture–coupled patch antenna array has been fabricated. The structure is presented in Fig. 3. The antenna is composed of two layers: a substrate with feeding and switching networks, and a superstrate with radiating elements. Advantages of this TMAA design are moderate size and electrical separation between patches and switches.

The substrate is made of $1\,\mathrm{mm}$ thick FR4 laminate. The feed network with four GaAs FET SPDT nonreflective switches is placed on the bottom side, and a conductive plane with eight slots is placed on the top side. The feed network is designed in such a way that the linear array 1 and the linear array 2 are excited from opposite edges. In this simply way, the $180°$ phase compensation is implemented. The superstrate is made of $1.524\,\mathrm{mm}$ thick RO4003C$^{\mathrm{TM}}$ laminate with eight patch radiators edged on the top. The bottom layer is non–metalized.

The ON/OFF switching is controlled through two enclosed digital delay generators (DDG) with $10\,\mathrm{ps}$ delay resolution. Such short delays provide phase–shift resolution on sidebands of less than $0.01°$. Clocks of both DDGs are synchronized using a microcontroller with $1\,\mathrm{MHz}$ triggering frequency; hence, sideband components appear with $1\,\mathrm{MHz}$ spacing.

III. Measurements

A. Radiation pattern of static array

Firstly, the antenna was measured in a „static“ mode without time–modulation, i.e. when only one line of patches is active. The gain for each linear array, without time–modulation, was measured around $8\,\mathrm{dBi}$. Radiation patterns for both linear arrays are similar.

B. Radiation patterns of harmonic beams

Usually, an antenna is excited and measured at the same frequency f_0, giving scattering parameters s_{11} for the reflection coefficient and s_{21} for the transmission coefficient. For this reason, vector network analyzer (VNA) is an instrument commonly used in an anechoic chamber for antenna testing. However, the measurement of sideband components requires a more sophisticated setup. Such measurement can be realized with a signal generator and a spectrum analyzer; it can, however, be also achieved with appropriately configured VNA.

Our measurement method involves a 4–port VNA with two independent RF sources at Port 1 and Port 3. A diagram of the measurement setup is presented in Fig. 4. Port 1 is used to excite the reference antenna at a fixed frequency $f_0 = 2.6\,\mathrm{GHz}$. Port 3 is used to analyze a signal received with the TMAA. The oscillator related to Port 3 sweeps the frequency with a step of $f_p = 1\,\mathrm{MHz}$; thus, the VNA measures signal exactly on the carrier frequency and the sideband components. Power level measured at each component is compensated with propagation losses to obtain gain. The designed TMAA was measured in receiving mode on six different sidebands; in this

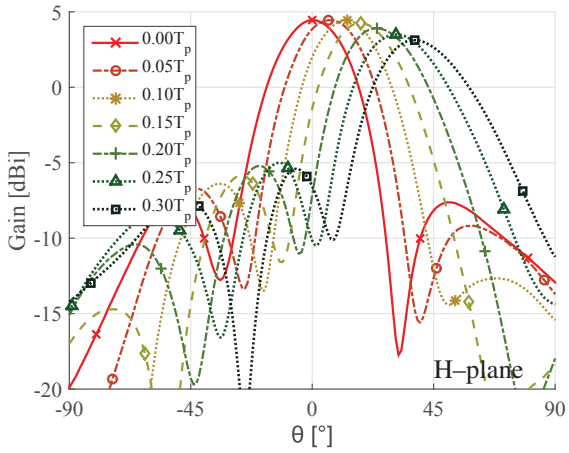

Fig. 5. Measured radiation pattern for the first positive sideband $h = 1$.

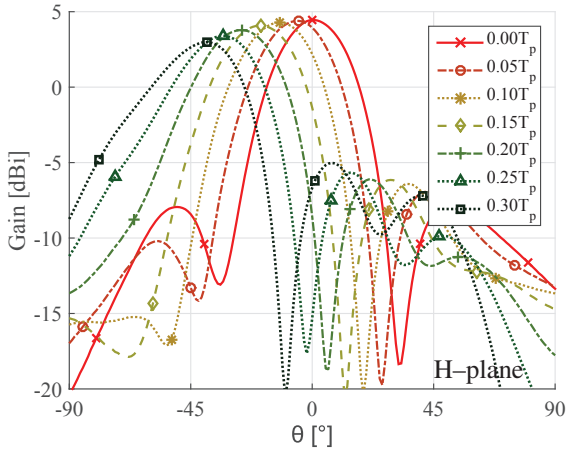

Fig. 6. Measured radiation pattern for the first negative sideband $h = -1$.

paper, however, we present only the most interesting results for $h = \pm 1$.

Radiation patterns for $h = 1$ and $h = -1$ are presented in Fig. 5 and Fig. 6, respectively. The maximum gain of $4.5\,\mathrm{dBi}$ is achieved for $\Delta t = 0$. The main lobes for $h = 1$ and $h = -1$ are scanning in opposite directions with increasing value of Δt. The greater is the delay the wider is the scanning angle. For $\Delta t = 0.25T_p = 250\,\mathrm{ns}$, the main lobe is scanned $40°$ away from the broadside direction with $1.5\,\mathrm{dB}$ drop in the gain.

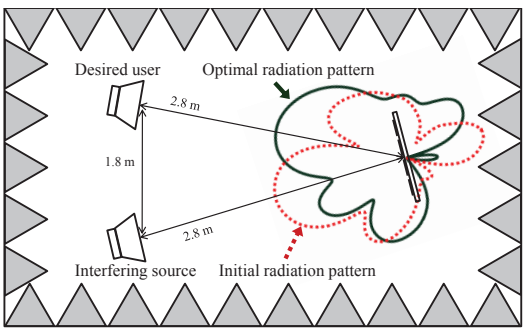

Fig. 7. Setup for experimental interference cancellation.

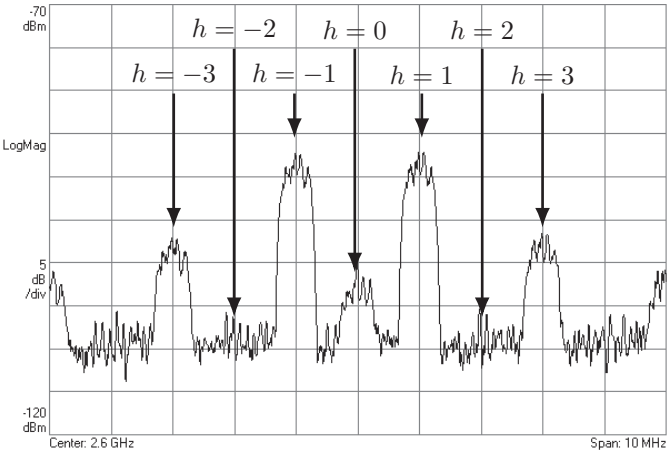

Fig. 8. Measured spectrum of the received signal after time–modulation.

C. Interference cancellation

The proposed TMAA was applied to a wireless communication system to verify its suitability in interference cancellation. The setup of the experiment is presented in Fig. 7. The test scenario was prepared as follows. A digitally modulated signal was transmitted to the receiving TMAA. This transmission was interrupted by a strong source of interference (IS). The TMAA was directed opposite to the IS; thus, the quality of the desired signal was disrupted. The aim was to adapt the radiation pattern by moving the main lobe towards the desired user, and eventually improve the signal–to–noise ratio (SNR) and the error vector magnitude (EVM) in the receiver.

The experiment was conducted in an anechoic chamber. The distance between the TMAA and transmitting antennas was approximately 24λ. The desired signal was generated using Rohde&Schwarz SMBV100A Vector Signal Generator as a 16–QAM signal with $500\,\mathrm{ksym/s}$ throughput, carrier frequency $f_0 = 2.6\,\mathrm{GHz}$, and power $10\,\mathrm{dBm}$. The interfering signal was generated using Rohde&Schwarz SMF100A Signal Generator as a Gaussian noise with $400\,\mathrm{kHz}$ of occupied bandwidth and power $-10\,\mathrm{dBm}$.

The receiving part comprises the TMAA connected to the Agilent E4440A PSA Series Spectrum Analyzer with Agilent 89600 Vector Signal Analyzer Software, which served as a digital demodulator and a signal quality tester. The spectrum of the signal received from the TMAA is presented in Fig. 8. A low–level leakage of the carrier component ($h = 0$) is caused by fabrication inaccuracy. The linear array 1 and the linear array 2 should have $180°$ phase–difference due to the excitement from opposite edges. However, the measured phase–difference is around $170°$ which causes this leakage. Nevertheless, with perfect fabrication, the carrier component would disappear completely.

Firstly, a reference measurement for a single linear array without time–modulation was performed. The radiation pattern for the non–modulated array is drawn with a dotted line in Fig. 7. For this case, the main lobe is directed towards the IS and the first null of the radiation pattern is directed towards the desired user; thus, the signal with QAM–16 modulation is substantially disturbed. Baseband symbols of the received

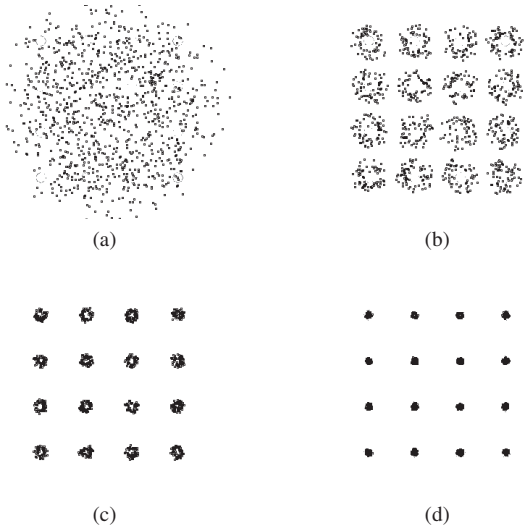

Fig. 9. Measured baseband symbols of signal received with TMAA for a) static linear array, and TMAA with b) $\Delta t = 0.09T_p$, c) $\Delta t = 0.13T_p$, and d) $\Delta t = 0.19T_p$.

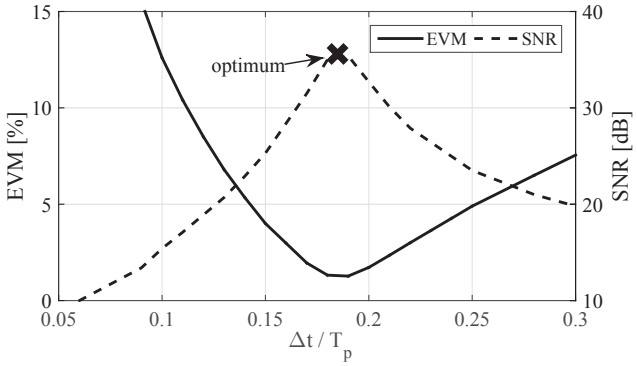

Fig. 10. Measured improvement of the EVM and the SNR.

signal are presented in Fig. 9a. Its distribution does not correspond to the required QAM–16 constellation.

During the second experiment the time–modulation was activated and the physical setup remained unchanged. The adaptation of the radiation pattern was achieved by increasing a value of Δt with $10\,\mathrm{ns}$ step starting from 0. The VSA was set to demodulate the signal from the first negative sideband; thus, $f_{VSA} = 2.599\,\mathrm{GHz}$. The SNR and the EVM improvement is plotted in Fig. 10 and the distribution of baseband symbols for selected steps of adaptation is presented in Fig. 9b, Fig. 9c, and Fig. 9d. The adaptation reached the optimum value of the SNR $= 35\,\mathrm{dB}$ and the EVM $= 1.3\,\%$ for $\Delta t = 0.19T_p$. At this point, the main lobe of the radiation pattern for $h = -1$ is directed towards the desired user, even if the antenna is physically directed opposite to the IS. The shape of the optimum radiation pattern is drawn with a solid line in Fig. 7.

IV. Conclusion

In this paper, a novel architecture for a TMAA with beam–scanning has been proposed. The concept has been implemented by placing low–cost SPDT GaAs switches in the feed network of the aperture–coupled patch antenna array. The proposed TMAA has three major advantages. Firstly, the switching network is lossless in this sense that there is no power loss during the OFF state, which improves the efficiency. Secondly, the TMAA provides harmonic beam–scanning on odd sideband components. The main beam on the first sideband can be continuously scanned more than $30°$ from the broadside direction without significant loss in the gain. Thirdly, the maximum bandwidth of a transmitted signal is doubled because even siedebands and the carrier component are eliminated. The developed TMAA has been verified as a part of a wireless digital communication system and provided more than $25\,\mathrm{dB}$ improvement in the SNR . The new approach reported in this paper demonstrates that the proposed TMAA may be a promising candidate for a low–cost active antenna for wireless communication systems.

References

[1] W. Kummer, A. Villeneuve, T. Fong, F. Terrio, "Ultra–low sidelobes from time–modulated arrays," *IEEE Trans. Antennas Propag.*, vol. 11, no 6, pp. 633–639, 1963.

[2] H. Shanks, "A New Technique for Electronic Scanning," *IRE Trans. Antennas Propag.*, vol. 9, no 2, pp. 162–166, 1961.

[3] L. Poli, P. Rocca, G. Oliveri, A. Massa, "Harmonic Beamforming in Time-Modulated Linear Arrays," *IEEE Trans. Antennas Propag.*, vol. 59, no 7, pp. 2538–2545, July 2011.

[4] M. Thian V. F. Fusco, "Ultrafast Low–Loss 42–70 GHz Differential SPDT Switch in 0.35um SiGe Technology," *IEEE Trans. Microw. Theory Tech.*, vol. 60, no 3, pp. 655–659, 2012.

[5] Y. Yashchyshyn, K. Derzakowski, P. Bajurko, J. Marczewski, S. Kozowski, "Time–Modulated Reconfigurable Antenna Based on Integrated S–PIN Diodes for mm–Wave Communication Systems," *IEEE Trans. Antennas Propag.*, vol. 63, no 9, pp. 4121–4131, Sept 2015.

[6] S. Yang, Y. B. Gan, P. K. Tan, "Evaluation of directivity and gain for time-modulated linear antenna arrays," *Microw. Opt. Technol. Lett.*, vol. 42, no 2, pp. 167–171, 2004.

[7] J. Brégains, J. Fondevila-Gomez, G. Franceschetti, F. Ares, "Signal Radiation and Power Losses of Time-Modulated Arrays," *IEEE Trans. Antennas Propag.*, vol. 56, no 6, pp. 1799–1804, 2008.

[8] A. Tennant B. Chambers, "A Two-Element Time-Modulated Array With Direction-Finding Properties," *IEEE Antennas Wireless Propag. Lett.*, vol. 6, pp. 64–65, 2007.

[9] P. Rocca, L. Poli, G. Oliveri, A. Massa, "Adaptive Nulling in Time-Varying Scenarios Through Time-Modulated Linear Arrays," *IEEE Antennas Wireless Propag. Lett.*, vol. 11, pp. 101–104, 2012.

[10] G. Bogdan, P. Bajurko, Y. Yashchyshyn, "Null–steering in two–element time modulated linear antenna array through pulse–delay approach," in *Proc. 20th Int. Conf. Microw. Radar Wireless Commun. (MIKON)*, June 2014, pp. 1–4.

[11] P. Rocca, Q. Zhu, E. Bekele, S. Yang, A. Massa, "4-D Arrays as Enabling Technology for Cognitive Radio Systems," *IEEE Trans. Antennas Propag.*, vol. 62, no 3, pp. 1102–1116, 2014.

[12] Y. Tong A. Tennant, "A Two–Channel Time Modulated Linear Array With Adaptive Beamforming," *IEEE Trans. Antennas Propag.*, vol. 60, no 1, pp. 141–147, 2012.

[13] Q. Zhu, S. Yang, R. Yao, Z. Nie, "Gain Improvement in Time-Modulated Linear Arrays Using SPDT Switches," *IEEE Antennas Wireless Propag. Lett.*, vol. 11, pp. 994–997, 2012.

[14] A.-M. Yao, W. Wu, D.-G. Fang, "Single-Sideband Time-Modulated Phased Array," *IEEE Trans. Antennas Propag.*, vol. 63, no 5, pp. 1957–1968, May 2015.

[15] P. Rocca, L. Poli, A. Massa, "Instantaneous directivity optimisation in time-modulated array receivers," *IET Microwaves Antennas Propag.*, vol. 6, no 14, pp. 1590–1597, 2012.

[16] R. Maneiro-Catoira, J. Brégains, J. Garcia-Naya, L. Castedo, "On the Feasibility of Time-Modulated Arrays for Digital Linear Modulations: A Theoretical Analysis," *IEEE Trans. Antennas Propag.*, vol. 62, no 12, pp. 6114–6122, Dec 2014.